Article

Proof of Concept of an Irradiance Estimation System for Reconfigurable Photovoltaic Arrays

Vincenzo Li Vigni, Damiano La Manna, Eleonora Riva Sanseverino *, Vincenzo di Dio, Pietro Romano, Pietro di Buono, Maurizio Pinto, Rosario Miceli and Costantino Giaconia

Department of Energy, Information Engineering and Mathematical Models (DEIM), University of Palermo, Viale delle Scienze, Edificio 9, Palermo 90128, Italy; E-Mails: vincenzo.livigni@unipa.it (V.L.V.); damiano.lamanna@unipa.it (D.L.M.); vincenzo.didio@unipa.it (V.D.); pietro.romano@unipa.it (P.R.); pietro.dibuono@unipa.it (P.B.); maurizio.pinto@unipa.it (M.P.); rosario.miceli@unipa.it (R.M.); costantino.giaconia@unipa.it (C.G.)

* Author to whom correspondence should be addressed; E-Mail: eleonora.rivasanseverino@unipa.it; Tel.: +39-091-238-60262; Fax: +39-091-488-452.

Abstract: In order to reduce the mismatch effect caused by non-uniform shadows in PV arrays, reconfigurable interconnections approaches have been recently proposed in the literature. These systems usually require the knowledge of the solar radiation affecting every solar module. The aim of this work is to evaluate the effectiveness of three irradiance estimation approaches in order to define which can be well suited for reconfigurable PV arrays. It is presented a real-time solar irradiance estimation device (IrradEst), implementing the three different estimation methods. The proposed system is based on mathematical models of PV modules enabling to estimate irradiation values by sensing a combination of temperature, voltage and current of a PV module. Experimental results showed generally good agreement between the estimated irradiances and the measurements performed by a standard pyranometer taken as reference. Finally one of the three methods was selected as possible solution for a reconfigurable PV system.

1. Introduction

In a photovoltaic field, when one or more modules belonging to a set of series-connected PV modules are shaded, the maximum generated current gets reduced, thus decreasing the output power for the whole string. Besides, a module or modules that are shaded or faulty can reach a too high temperature, related to the hotspot phenomenon, eventually leading to module breakdown. Hotspot and mismatch events can be controlled through bypass diodes, leaving out the shaded panel from the series and giving up entirely the energy of that panel, which could nonetheless provide its fair share of energy. Bypass diodes give rise to losses and local maxima in the PV curve, so the MPPT algorithm controlling the converter operation can be misled and local maximum operating points can be taken as absolute maximums.

In order to improve unequally irradiated PV plants performances, several strategies have been proposed in the literature, concerning conversion systems' architecture, different plant topologies or PV array reconfiguration [1]. To take into account non-uniform radiation conditions, many conversion system architectures are normally adopted by the designers. When sun exposure of the modules is uniform, a single (centralized) inverter can be used in small-medium PV plant. In other cases, when non uniform working conditions are more likely, string inverters or micro inverters are used instead [2–4]. Moreover performances of an unequally irradiated PV plant can be improved by different connection topologies of the PV plant. In the literature, [5,6], these topologies have been presented: Series-Parallel (SP), Total-Cross-Tied (TCT), Bridge-Linked (BL) and Honey Comb (HC). Series-parallel is the most common, simple and cheap connection, while the other topologies reduce the overall mismatch effect but they involve redundant connections thus higher costs. Therefore, some of them have been practically realized, whereas others are still at research exploitation level.

Very recently, based on any of the proposed above topologies, many promising techniques for dynamic reconfiguration systems have been presented enabling to compensate the mismatch effect. In fact, several authors have presented new approaches to increase the modules' power output under shading conditions [7], by measuring or estimating the PV modules radiation and changing the electrical interconnections between them.

For instance, in [8] it is shown an energy increase of PV arrays up to 30% of the total energy. In [9], experimental results prove that by using the reconfiguration system and an additional DC/DC converter, 13% of the power losses under partial shading can be recovered. Most PV reconfiguration techniques identify the irradiance value of each PV module of the plant and use this information as input for the relative optimization algorithm.

Furthermore, monitoring systems [10–15] are often needed in PV plants for collecting power production and performance data [16–18] as well as weather information. In this way, it is possible to track the working conditions of each module recognizing faulty units [19,20], preventing mismatch [21] and partial shading, avoiding significant power losses [22] through suitable control actions.

The most common method to sense the irradiance is by means of a pyranometer, thus common solar plants usually have one or a few such units for monitoring purposes. In order to have a good understanding of the spatial irradiance profile, one pyranometer per PV module should be used, thus giving raise to increased costs. Even if lower cost solutions exist, such as photo-diodes and photo-resistors, these, like the pyranometer, provide the irradiance information about their limited sensor area only, not for the full PV module surface.

Another approach enables to estimate the radiation level of each solar module by measuring its electrical characteristics [23]. Voltage, current and temperature can be used in combination with the physical parameters of the solar module to obtain the radiation value using the PV electrical model [24]. As an example, the irradiation equalization algorithm proposed in [25] for a TCT topology, requires the knowledge of the radiation for every PV module; while in [26] the voltage-current sensing is taken into account to estimate the irradiance. Otherwise, in [27] the radiation equalization strategy was applied to asymmetric PV matrix. A further approach is suggested by [28], named "adaptive bank"; it is based on the measure of the operative voltage, open-circuit voltage and module temperature. In [29] the authors proposed an "elastic" PV structure, acquiring voltage, current and the temperature of all modules, organized in a SP topology. The reconfiguration strategy proposed in [30], instead, estimates the irradiance by measuring cell temperature, bypass-diode current and short-circuits current. In [31] a simplified model to estimate the irradiation, starting from the module's voltage and current, has been used. However, since the irradiance estimated by the mathematical model usually requires the temperature parameter, in many real-world cases, temperature effects should not be neglected. In fact, under shadowing conditions, the temperature's difference, ΔT between different modules can be significantly greater than zero. Thus, the radiation levels can be considerably different, due to the temperature difference ΔT, even if the modules show similar values of voltages and currents.

In this paper, three different irradiance estimation methods are explored using a purposely designed real-time solar irradiance estimation system (IrradEst). The three approaches (with panel under load, short circuit or open circuit) are compared in order to define which is well suited for applications on reconfigurable PV arrays. The IrradEst implements the mathematical models of PV modules enabling to estimate irradiation values by sensing a combination of temperature, voltage and current values of the PV module. Some characteristics of the PV module are requested by the mathematical model and can be provided mainly by its datasheet. The instrument in turn provides, in real-time, the information of the sensed parameters for further monitoring and data logging purposes.

In Section 2, the PV mathematical model and the fundamental relations that are used in the presented system are discussed. Section 3 shows the architecture of the proposed system and its realization, while in Section 4 the experimental setup and major results are reported. Finally, conclusions and future developments are explored in Section 5.

2. Photovoltaic Mathematical Model

Many mathematical models describing the photovoltaic cell have been proposed in the literature [32–35]. Depending on the number of the parameters used to model the solar cell, the accuracy improves while computational complexity increases. The three estimation methods of the IrradEst are derived form a 5-parameter model [36], this being a good compromise between accuracy and calculation times, compatible with an elaboration on a Microcontroller Unit (MCU). The single diode circuit model is shown in Figure 1.
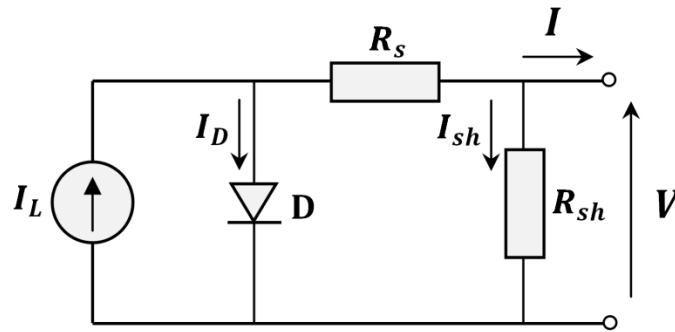
Figure 1. Electrical circuit of thesolar cell 5-parameter model.

In a commercial PV module, several photovoltaic cells are series-connected in order to achieve the desired voltages. The total module current I is expressed by Equations (1) and (2):

$$I = I_L - I_D - I_{sh} \tag{1}$$

where I_D is the diode current and it is given by:

$$I_D = I_0 \left(\exp\left(\frac{V + IR_s}{N_s A V_t} \right) - 1 \right)$$

Substituting this Equation in Equation (1):

$$I = I_L - I_0 \left(\exp\left(\frac{V + IR_s}{N_s A V_t} \right) - 1 \right) - \frac{V + IR_s}{R_{sh}} \tag{2}$$

where

I_L is the light-generated current,

I_0 the diode reverse saturation current,

R_s and R_{sh} respectively the cell series and shunt resistance,

N_s the number of cells series-connected,

A the ideality factor,

V_t is the thermal voltage which can be calculated as kT_c/q, where k is the Boltzmann's constant, q the electron charge and T_c the temperature of cell.

It should be noted that Equation (2) is a transcendental equation and parameters have to be quantified considering their dependence on solar radiation and temperature [37,38]. In particular, I_0 and I_L are temperature-dependent, as shown in Equations (3) and (5):

$$I_0 = I_{d0} \left(\frac{T_c}{T_{C_{STC}}} \right)^3 \exp\left[\frac{qE_g}{Ak} \left(\frac{1}{T_{C_{STC}}} - \frac{1}{T_c} \right) \right] \tag{3}$$

where I_{d0} is the reverse saturation current in STC, E_g is the band gap energy:

$$E_g = 1.16 - 7.02 \times 10^{-4} \frac{T_c^2}{T_c + 1108} \tag{4}$$

the light-generated current can be expressed by:

$$I_L = \left(\frac{G}{G_{STC}} \right) \left[I_{L_{STC}} + \mu_{I_{SC}}(T_c - T_{C_{STC}}) \right] \tag{5}$$

where G is the solar radiation measured in $\frac{W}{m^2}$, G_{STC} the solar radiation in standard conditions, STC$\left(1000 \frac{W}{m^2}\right)$, $T_{C_{STC}}$ the temperature at STC (298.15 K), $\mu_{I_{SC}}$ is the short-circuit current temperature coefficient. $I_{L_{STC}}$ is the PV cell light-generated current at STC.

Substituting Equation (5) in Equation (2), the following expression is obtained:

$$G = \frac{G_{STC}}{I_{L_{STC}} + \mu_{1_{SC}}(T_c - T_{C_{STC}})} \left[I + I_0 \left(e^{\frac{V+IR_s}{N_s A k \frac{T_c}{q}}} - 1 \right) + \frac{V + IR_s}{R_{sh}} \right] \tag{6}$$

Knowing all model parameters and measuring voltage, current and temperature at each module allows to derive from Equation (6) an estimate of the irradiation. However, obtaining the model parameters that meet the electrical characteristic of the real panel in all its operating points can be quite tedious. In order to reduce the model parameters sensitivity and obtain a better estimation of the irradiation, it can be useful to force the working point of the panel to short-circuit or open circuit conditions. In this case, Equation (6) can be simplified as:

$$G_{V_{oc}} = G_{STC}\, e^{\frac{V_{oc} - V_{oc_{STC}} - \mu_{V_{oc}}\left(T_c - T_{c_{STC}}\right)}{N_s A k \frac{T_c}{q}}} \tag{7}$$

$$G_{I_{sc}} = \frac{G_{STC}}{I_{SC_{STC}}}\left(I_{sc} - \mu_{I_{sc}}\left(T_c - T_{c_{STC}}\right)\right) \tag{8}$$

where $\mu_{V_{oc}}$ is the open-circuit voltage temperature coefficient and $I_{SC_{STC}}$ the short-circuit current in STC.

It should be noted that I_0, R_s and R_{sh} must be first obtained using the iterative method discussed in [39], providing the data found on the technical datasheet of the PV module. If the PV plant is formed by solar modules all of the same model, this calculation is performed one time only. Also, it worth noting that R_s and R_{sh} have dependence from the temperature. However, in the actual operating temperature range of a PV module, the variations are about 10 mΩ for R_s and 100 Ω per R_{sh}, and can be neglected in our application.

In Equations (7) and (8) only two parameters are needed to evaluate the solar radiation received by the PV module. In the first case it is necessary acquiring open circuit voltage V_{oc} and cell temperature, while, in the other, short circuit current I_{sc} and the solar cell temperature.

Although the presented equations are valid only for normal incidence angles, it should be taken into account that, for the purposes of array reconfiguration, the knowledge of real irradiance on the area where the panel insists is not important. In fact, the calculated irradiance does not refers to the incident energy on the panel, but to the radiation (purged from the amount of energy that is lost at the interface or because of the module degradation) which can be truly harvested from the panel.

3. Irradiance Estimation System—IrradEst

In this section, the main aspects of the presented irradiance estimation system are presented. This prototype has been implemented for testing on the field the irradiance estimation methods described in Section 2. In fact, IrradEst enables to autonomously acquire voltage, current and temperature of a solar module, alternating three different conditions, *i.e.*, open circuit, short circuit and under load, computing

in firmware Equations (6)–(8), eventually providing the estimated irradiance values to the user. The total cost of this prototype is around 15 EUR while the power consumption is below 1 W. The block diagram of the device is shown in Figure 2 and it will be discussed in this section.
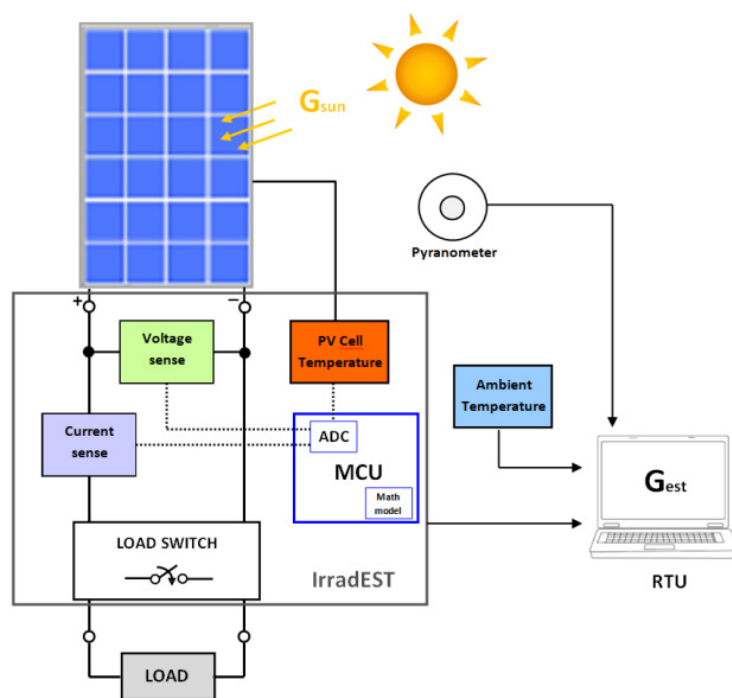

Figure 2. Block diagram of the measuring setup.

3.1. Conditioning Circuit

Three conditioning circuits were implemented for measuring voltage, current and temperature of the module. Since the voltage of a solar module is usually at higher level of the common supply voltage of the electronics (5 V in our design), a voltage divider in combination with an instrumentation amplifier was used. The voltage across the PV module leads was reduced and then differentially amplified. The analog to digital conversion was performed by one the ADC channels embedded into the microcontroller.

A relatively non-expensive Hall-effect sensor was selected for sensing the current. Such a sensor can measure up to ± 12.5 A providing an output voltage of 110 mV/A and a quiescent voltage centered in the middle of the supply voltages. Amplification was not necessary and the output of the sensor was directly connected to another ADC channel of the MCU.

The temperature of the solar module was sensed by a standard Integrated Circuit (IC) temperature sensor LM35, providing ± 0.5 °C accuracy at 25 °C. Since this 3-pin IC has to be glued behind a solar cell of the module, a three-wire cable running from the module to the monitoring device was required. Also in this case, no amplification was necessary and a low-pass RC-filter connects the temperature sensor output to the MCU ADC channel. Another temperature sensor was also used to sense the external temperature.

It should be noted that the LM35 glued on the back of the solar cell is actually providing the temperature of the back of the cell T_{back} and not T_c. In [39] is reported that $T_c = T_{back} + \left(\frac{G}{G_{stc}}\right)\Delta T$ (where G is the measured irradiance, $G_{stc} = 1000$ W/m^2 and ΔT the difference between T_{back} and T_c at G_{stc}). Since the differences between T_c and T_{back} measured during the tests were negligible, we could

approximate T_{cell} to T_{back} in order to avoid the recursive dependence from G. Also we assume that if the radiance is uniform on the solar module, the temperature of one cell can be representative for all the modules.

3.2. Measuring Switches

Two measuring switches were enabled or disabled by the MCU using two transistors as drivers, performing the three different switch configurations, *i.e.*, open circuit, short circuit and under load. The first switch, henceforth K1, implemented the short-circuit configuration, connecting the two PV module leads together; the second switch, K2, disconnected the solar module from the load enabling the open-circuit configuration. This enabled sensing open-circuit voltage V_{oc} as well as short-circuits current I_{sc}, in addition to voltage V_L and current I_L under given load conditions.

3.3. Microcontroller

The MCU continuously acquired the values of the three configured ADC channels, saving data to the local memory. Using this information, the 8-bit MCU calculated in a negligible time the irradiance estimations by using the expressions Equations (6)–(8) provided by the model described in Section 2. The acquired data were remotely read from a PC connected by means of a USB cable. The IrradEst system can be also attached to an Android smartphone by means of an USB On-The-Go (OTG) cable in order to easily interact with the system (e.g., read electrical variables, open or close the measuring switches) without using a host PC. The IrradEst can be powered by the USB bus or by an external battery.

4. Experimental Tests and Results

In order to validate the three irradiance estimation approaches, the IrradEst was connected to a solar module. In particular the Kyocera 175GHT2 was readily available and the parameters to fulfill the Equations (6)–(8) were obtained, by using the iterative method on Matlab proposed in [40,41], and loaded into the microcontroller of the IrradEst. The main idea was to compare the estimated values of irradiance calculated by the IrradEst, to the irradiance measured by a standard pyranometer taken as reference and placed near the solar module under test.

4.1. Description of the Experimental Setup and Procedures

The voltage and current readings of the IrradEst were calibrated using a multimeter, while the temperature of the solar module and the external one were calibrated respectively with two PT100 sensors. As load, a potentiometer was connected to the output of the IrradEst and its resistance value was chosen during tests in order to set the solar module in its maximum power point. This procedure was performed configuring the IrradEst on under-load condition: The instrument continuously provided the measured power as output to the serial terminal on the PC. The potentiometer value was set when the power value was the maximum.

4.2. Test Explanation

During the tests, the IrradEst was connected to a PC and interfaced by means of a serial terminal program. The pyranometer and the two PT100s used to sense the ambient and PV module temperatures were connected to their respective data logger. The pyranometer shows limited differences from solar polycrystalline modules in terms of solar spectral effects as pointed out in [42] therefore in this work no corrective term is considered in the model. However these effects should be further elaborated and taken into account, since in presence of variable shading and tilting of the module the spectral distribution is less likely to be constant. At the end of the test, all the data was downloaded on the laptop for further analysis. The complete measurement equipment is reported in Table 1 and the experimental setup is shown in Figure 3.

Table 1. Measurement setup.

Solar module	Kyocera 175GHT2
Pyranometer-Data Logger	Kipp and Zonen CMP 3
Ambient Temperature	Delta Ohm TP 472 PT 100
Cell Temperature	Delta Ohm TP 878.1 PT 100
Temperature Data Logger	Delta Ohm DO9847
Multimeter	Fluke 89 IV
Potentiometer	0–10 Ω, supporting currents up to 10A

Figure 3. Experimental setup using a PV module Kyocera 175GHT2.

In order to compare the different radiation estimations provided by Equations (6)–(8), the three conditions of short-circuit, open-circuit and under-load were obtained at every MCU iteration. In particular, the MCU followed these steps in an infinite loop:

(1) K1 and K2 switches were closed in order to set the PV module in short-circuit and current I_{sc} was acquired;

(2) K1 switch was opened so that the load is not bypassed and the under-load voltage V_L, current I_L and cell temperature T_i were measured;

(3) K1 and K2 switches were opened so that load was disconnected and open-circuit voltage V_{oc} was sensed.

(4) The estimated radiations were calculated:

    (a) G_{Isc} calculated by Equation (8) using I_{sc} and T_i;

    (b) G_{load} calculated by Equation (6) using V_L, I_L and T_i;

    (c) G_{Voc} calculated by Equation (7) using V_{oc} and T_i;

(5) The acquired data and the estimated irradiances were sent to the host PC. New data was provided every 15 s (the acquisition period can be adjusted).

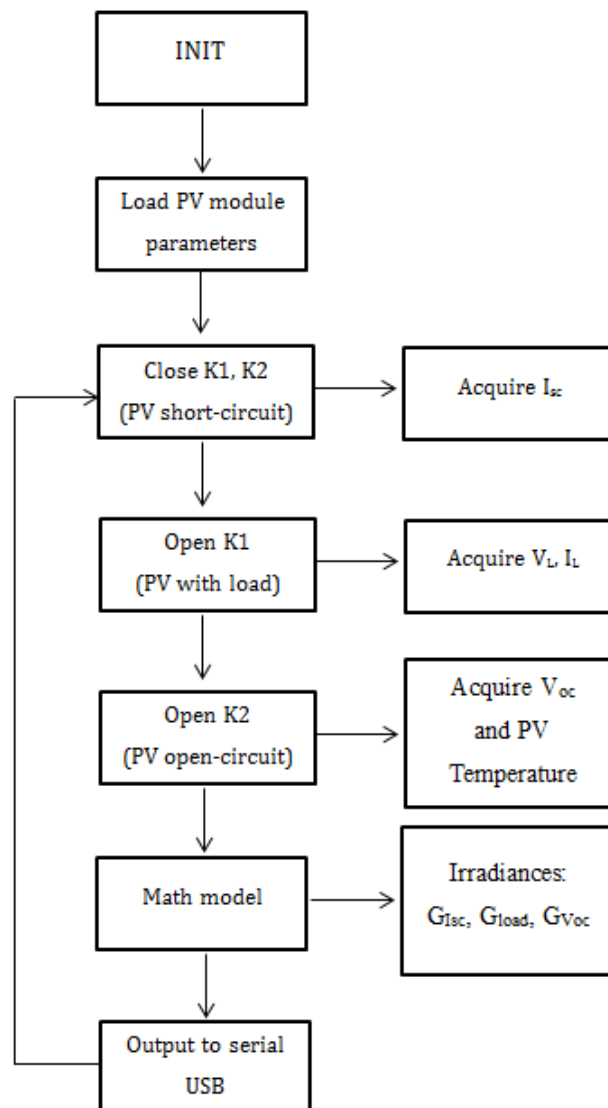The flowchart of the algorithm is shown in Figure 4.

Figure 4. Flow-chart of IrradEst firmware.

4.3. Analysis of the Experimental Results

Figure 5a shows the temporal diagram of a half-hour acquisition, taken during a partly cloudy day in Palermo, Italy. In this chart, the radiation acquired by the pyranometer (black) and those estimated by the MCU (colored) are reported. It should be noted that in the first part of the acquisition ($t < 700$ s) the solar radiation value remained constant and equal to 920 W/m^2. At this point, the PV module under test was artificially shaded using a covering plastic sheet. Considering Figure 5, in the first two time intervals, circled in figure, the PV module was shaded with one layer of plastic sheet, while in the third time interval, the shadow was made with two layers of sheets (see the zoomed time interval in Figure 5b) in order to have a deeper shadow effect. Instead, in the second part of the acquisition for $t > 700$ s, the solar radiation variation was given by natural passing clouds (Figure 5c).
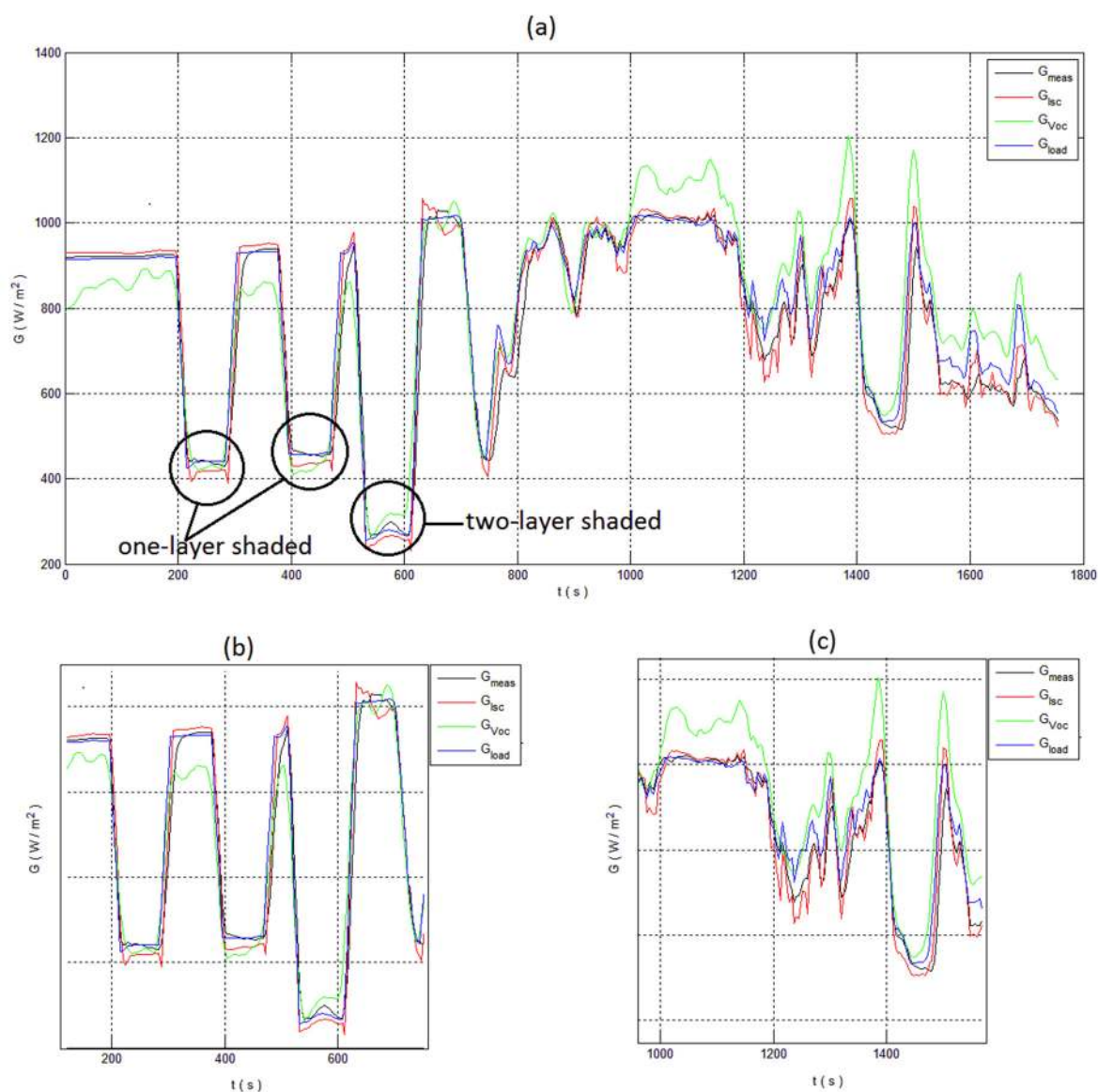

Figure 5. (**a**) Chart of the half-hour measure, showing the trend of G$_{meas}$, G$_{Isc}$, G$_{Voc}$ and G$_{load}$; (**b**) the artificial shading incidence caused by one or two layers shaded; (**c**) a zoomed view of the most variable time interval of the measurement session highlights the high difference among G$_{meas}$, G$_{Isc}$, G$_{Voc}$ and G$_{load}$.

In Table 2 the statistical error analysis of the measured and estimated irradiance is shown. In particular, the G_{Isc} and G_{load} values had a mean error respect to G_{meas} W/m^2 of 48 and 55 W/m^2 respectively, while G_{Voc} results in a higher error mean (87 W/m^2) and standard deviation. This is mainly due to the low sensitivity of the panel voltage to the irradiance, as shown in the exponential function of the mathematical model Equation (7), where very low changes of voltage or cell temperature are virtually amplified. Of course, better accuracy could be obtained using a higher resolution voltage measurement. Conversely, G_{Isc} is very close to G_{meas} because of the linear relationship between the incident radiation and the short-circuit current of PV module, as in Equation (8). The e_{mean}% deviation for G_{Isc} and G_{load} did not exceed the 7% of the G_{meas} value.

Table 2. Statistical analysis for all estimation methods: Mean error, standard deviation and percentage error of the solar radiation *vs.* G_{meas}.

Methods	$e_{mean}\left(\dfrac{w}{m^2}\right)$	$\sigma\left(\dfrac{w}{m^2}\right)$	e_{mean} %
Short-circuit	48	58	6.4
Load	55	64	6.8
Open-circuit	87	8	11.3

Good results were achieved by the under-load estimation. In fact, G_{load} closely followed G_{meas}, providing an average error equal to 55 W/m^2 and standard deviation of 64 W/m^2. This accuracy is appropriate in a reconfigurable PV controlling system, where a value of 100 W/m^2 is a reasonable threshold for the algorithm to change the switching configuration. Furthermore, during the tests it was noted that minimum errors were registered when the PV module was working near the Maximum Power Point (MPP) of its characteristic curve. In the opinion of the authors this is due to the simplified mathematical model used in this approach, where a more accurate model could reduce the error, slightly increasing the computational cost.

With the data acquired during the tests it was performed a sensitivity analysis of the estimated irradiances in dependence of their main parameters. In particular the sensitivity was defined as:

$$S(G,P) = \left| \max\left(\frac{\Delta G}{\Delta P}\frac{P}{G}\right) \right| \tag{9}$$

where ΔG is the variation of the irradiance when a perturbation on the variable P is applied, ΔP is the perturbation of the variable P (*i.e.*, voltage, temperature or current), G and P are respectively the estimated irradiance and the variable in absence of the perturbation. In particular, it was added a random perturbation within 1% of the maximum variable value. The analysis was carried out adding the perturbation to one variable per time, leaving the others unperturbed. The results are shown in Table 3. It was evident that in short-circuit condition the linear relationship between the irradiance and the current provides S (G_{isc}, I_{sc}) = 1.04 and S (G_{isc}, T) = 0.5. On the contrary, in the open-circuit condition, S (G_{voc}, V_{oc}) = 17 and S (G_{voc}, T) = 22 meaning that even small variations of V_{oc} and T produce wide variations in G_{voc}. As a result, the percentage error of the voltage and temperature has to be two orders less respect to the error it is desired from the estimated irradiance; this can be challenging especially for the temperature as it was seen in our tests. The analysis of the under-load approach showed that

S (G_{Load}, T) = 0.045, S (G_{Load}, V) = 0.06 and S (G_{Load}, I) = 0.98, resulting in a major dependence from the current and almost equal small dependence from temperature and voltage.

Table 3. Sensitivity analysis of the estimation approaches in dependence of their main parameters.

Variable	G_{isc}	G_{voc}	G_{Load}
V	-	17	0.06
I	1.04	-	0.98
T	0.5	22	0.045

4.4. Application to Reconfigurable PV Arrays

As discussed in Section 1, a reconfigurable PV array system requires an effective way for estimating the working conditions of all the solar modules. In the literature on reconfigurable PV arrays [1], irradiance estimation is generally used for this scope. A reconfigurable PV system taking advantages of the IrradEst principles could be implemented as shown in Figure 6. In particular, the controlling algorithm of the reconfigurable PV arrays opportunely arranges the solar modules according to their irradiances. The optimization algorithm computes the optimized layout of PV modules to be implemented on the switching matrix.
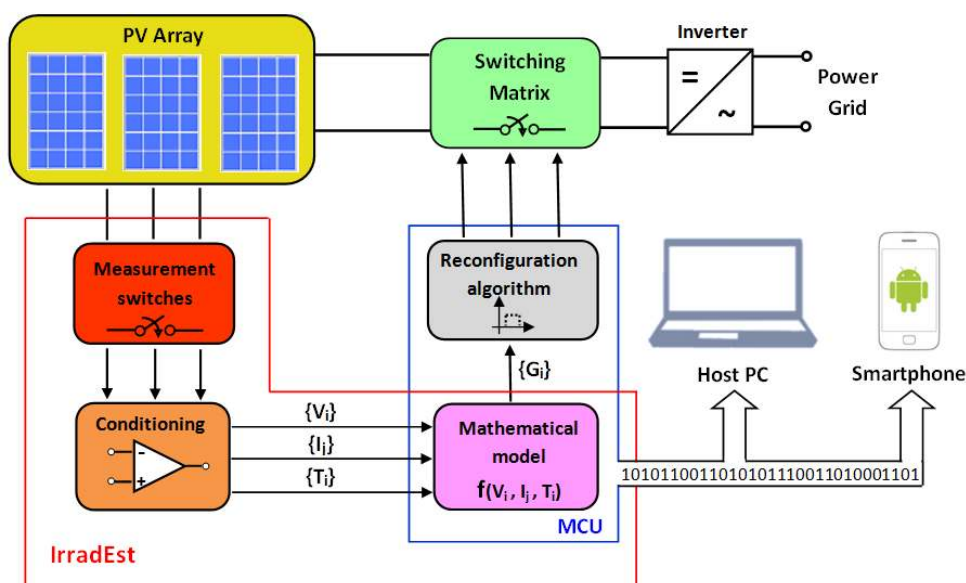

Figure 6. A reconfigurable PV system taking advantages of the irradiance estimations performed by the IrradEst.

As a result of the experimental tests performed with the IrradEst, the three different approaches analyzed in this paper enable to provide with a good accuracy the irradiance values needed by a reconfigurable array controller. Even if the short-circuit approach gives the most reliable information, this method requires the solar module to stop transferring power to the load during the measurement. On the contrary, the estimation performed under load conditions, even if not providing the most accurate irradiance estimation of three methods, does not need disconnecting the PV module from the input of the inverter. In the opinion of the authors, the accuracy of the estimation under these conditions enables its use on a reconfigurable PV array system. Furthermore, this estimation can be performed without

adding dedicated measuring switches, reducing power consumption and cost of the bill of material. If the only under load estimation is used, the "measuring switches" block in Figure 6 is no longer needed.

When several modules are connected together, the behavior of the bypass diodes must be considered. In particular, there are two possible solutions. If a system for the array reconfiguration is used, bypass diodes are not necessary, because the system itself is able to disconnect the panel from the array when the irradiance conditions are particularly unfavorable for the panel. Another solution could be to take in account the bypass diode in the panel model as in [43–45].

5. Conclusions

In this paper, three irradiance estimation approaches have been implemented on an irradiance estimation hardware system designed on purpose. The IrradEst takes advantage of the PV mathematical model in which the dependence of the irradiance by the voltage, current and temperature of the solar module is expressed. The first method works with the load connected to the PV module and uses the measurements of voltage, current and solar module's temperature to estimate the irradiance. The second method sets the PV module in open-circuit and calculates the solar irradiance estimated value by using the open-circuit voltage and temperature. The last estimation method uses the short-circuit current and the temperature. As results from the tests performed on a standard PV module connected to the IrradEst, whose estimated irradiances were compared to the one measured by a pyranometer taken as reference, the calculated values were in good agreement with the reference one. In particular it was noted the good accuracy of the short-circuit estimation, while the open-circuit method showed a less reliable estimation. The estimation performed with the load always connected to the PV module resulted to be the best compromise between accuracy and suitability in a reconfigurable PV system. In fact this method does not require to the user further dedicated measuring switches, thus decreasing power consumption and costs.

Further Developments

Further developments are directed to integrate this proof-of-concept in a custom reconfigurable PV system such in Figure 6. The optimization algorithm and the switching matrix are currently under final study. Another interesting application is a monitoring system derived from the IrradEst; this could be used to monitor the irradiances of all the PV modules in a solar plant (even not reconfigurable) as well as DC parameters and temperatures, providing important information about shadowing effects, possible electrical mismatches and health-state of the solar modules. In this scenario one simple unit per PV module is needed. The negligible power requested by each device could be harvested from the PV module itself using a DC-DC converter; its design has to be such that do not perturb the inverter operation, thus avoiding external power supplies or large batteries. The communication could be implemented by a radiofrequency (RF) link, *i.e.*, WiFi. All the data collected by such a system could be used as input to an advanced distributed MPPT algorithm (DMPPT) *i.e.*, the approaches described in [46].

Conflicts of Interest

The authors declare no conflict of interest.

References

1. La Manna, D.; Li Vigni, V.; Riva Sanseverino, E.; Di Dio, V.; Romano, P. Reconfigurable electrical interconnection strategies for photovoltaic arrays: A review. *Renew. Sustain. Energy Rev.* **2014**, *33*, 412–426.
2. Kim, K.A.; Lertburapa, S.; Xu, C.Y. Efficiency and cost trade-offs for designing module integrated converter photovoltaic systems. In Proceedings of the Power Energy Conference at Illinois (PECI), Champaign, IL, USA, 24–25 February 2012.
3. Elasser, A.; Agamy, M.; Sabate, J.; Steigerwald, R.; Fisher, R.; Harfman-Todorovic, M. A comparative study of central and distributed MPPT architectures for megawatt utility and large scale commercial photovoltaic plants. In Proceedings of the IECON 2010—36th Annual Conference on IEEE Industrial Electronics Society, Glendale, AZ, USA, 7–10 November 2010.
4. Zhang, Z.; Chen, M.; Chen, W.; Qian, Z.M. Design and Analysis of the synchronization control method for BCM/DCM current-mode flyback micro-inverter. In Proceedings of the 2013 Twenty–Eighth Annual IEEE, Long Beach Applied Power Electronics Conference and Exposition (APEC), CA, USA, 17–21 March 2013.
5. Ramos-Pajaet, C.A.; Bastidas, J.D.; Saavedra-Montes, A.J.; Guinjoan-Gispert, F.; Goez, M. Mathematical model of total cross-tied photovoltaic arrays in mismatching conditions. In Proceedings of the 2012 IEEE 4th Colombian Workshop on Circuits and Systems (CWCAS), Barranquilla, Colombia, 1–2 November 2012.
6. Villa, L.F.L.; Picault, D.; Raison, B.; Bacha, S.; Labonne, A. Maximizing the power output of partially shaded photovoltaic plants through optimization of the interconnections among its modules. *IEEE J. Photovolt.* **2012**, 154–163, doi:10.1109/JPHOTOV.2012.2185040.
7. Wang, Y.J.; Hsu, P.C. An investigation on partial shading of PV modules with different connection configurations of PV cells. *Energy* **2011**, *36*, 3069–3078.
8. Nguyen, D.; Boston, M.A.; Lehman, B. An Adaptive Solar Photovoltaic Array Using Model-Based Reconfiguration Algorithm. *IEEE Trans. Ind. Electron.* **2008**, *55*, 2644–2654.
9. Alahmad, M.; Chaaban, M.A.; Lau, S.K.; Shi, J.; Neal, J. An adaptive utility interactive photovoltaic system based on a flexible switch matrix to optimize performance in real-time. *Sol. Energy* **2012**, *86*, 951–963.
10. Husain, N.S.; Zainal, N.A.; Singh, B.S.M.; Mohamed, N.M.; Mohd Nor, N. Integrated PV based solar insolation measurement and performance monitoring system. In Proceedings of the Science and Engineering 2011 IEEE Colloquium on Humanities, Penang, Malaysia, 5–6 December 2011.
11. So, J.H.; Jung, Y.S.; Yu, G.J.; Choi, J.Y.; Choi, J.H. Performance results and analysis of 3kW grid-connected PV systems. *Renew. Energy* **2007**, *32*, 1858–1872.
12. Kang, M.S.; Kang, H.; Choi, E.C. Monitoring technology available for measuring multiple-photovoltaic panel arrays. In Proceedings of the TENCON Spring Conference, Sydney, Australia, 17–19 April 2013.

13. Rivai, A.; Rahim, N. A low-cost photovoltaic (PV) array monitoring system. In Proceedings of the 2013 IEEE Conference on Clean Energy and Technology (CEAT), Lankgkawi, Malaysia, 18–20 November 2013; pp. 169–174.

14. Prieto M.J.; Pernia, A.M.; Nuno, F.; Diaz, J.; Villegas, P.J. Development of a Wireless Sensor Network for Individual Monitoring of Panels in a Photovoltaic Plant. *Sensors* **2014**, *14*, 2379–2396.

15. Patnaik, B. Distributed multi-sensor network for real time monitoring of illumination states for a reconfigurable solar photovoltaic array. *Phys. Technol.* **2012**, doi:10.1109/ISPTS.2012.6260892.

16. Zou, X.; Li, B.; Zhai, Y.H.; Liu, H.T. Performance Monitoring and Test System for Grid-Connected Photovoltaic Systems. In Proceedings of the Asia-Pacific Power and Energy Engineering Conference (APPEEC), Shanghai, China, 27–29 March 2012.

17. Robinson Rodriguez, D.; Jutinico Alarcon, A.L.; Jimenez Moreno, R. Monitoring system for global solar radiation, temperature, current and power for a photovoltaic system interconnected with the electricity distribution network in Bogota. In Proceedings of the 56th International Midwest Symposium on Circuits and Systems, Columbus, OH, USA, 4–7 August 2013.

18. Chouder, A.; Silvestre, S.; Taghezouit, B.; Karatepe, E. Monitoring, modelling and simulation of PV systems using LabVIEW. *Sol. Energy* **2013**, *91*, 337–349.

19. Chao, K.H.; Ho, S.H.; Wang, M.H. Modeling and fault diagnosis of a photovoltaic system. *Electr. Power Syst. Res.* **2008**, *78*, 97–105.

20. Chouder, A.; Silvestre, S. Automatic supervision and fault detection of PV systems based on power losses analysis. *Energy Convers. Manag.* **2010**, *51*, 1929–1937.

21. Alonso-Garcia, M.C.; Ruiz, J.M.; Chenlo, F. Experimental study of mismatch and shading effects in the I–V characteristic of a photovoltaic module. *Sol. Energy Mater. Sol. Cells* **2006**, *90*, 329–340.

22. Maki, A.; Valkealahti, S. Power losses in long string and parallel-connected short strings of series-connected silicon-based photovoltaic modules due to partial shading conditions. *IEEE Trans. Energy Convers.* **2012**, *27*, 173–183.

23. Bonanno, F.; Capizzi, G.; Graditi, C.N.; Tina, G.M. A radial basis function neural network based approach for the electrical characteristics estimation of a photovoltaic module. *Appl. Energy* **2012**, *97*, 956–961.

24. Calò, P.; Fiscelli, G.; Lo Bue, F.; Di Stefano, A.; Giaconia, C. An Electronic Emulator of Combined Photovoltaic and Solar Thermal Systems. In Proceedings of the 2010 Fifth International Conference on Ecological Vehicles and Renewable Energies (EVER), Monaco, 25–28 March 2010.

25. Velasco-Quesada, G.; Negroni, J.J.; Guinjoan, F.; Pique, R. Radiation equalization method for output power optimization in plant oriented grid-connected PV generators. In Proceedings of the European Conference on Power Electronics and Applications, Dresden, Germany, 11–14 September 2005.

26. Wilson, P.; Storey, J. Improved optimization strategy for radiation equalization in dynamic photovoltaic arrays. *IEEE Trans. Power Electron.* **2013**, *28*, 2946–2956.

27. Romano, P.; Candela, R.; Cardinale, M.; Li, V.V.; Musso, D; Riva, S.E. Optimization of photovoltaic energy production through an efficient switching matrix. *J. Sustain. Dev. Energy Water Environ. Syst.* **2013**, *1*, 227–236.

28. Nguyen, D.D. Modeling and reconfiguration of solar photovoltaic arrays under non-uniform shadow conditions. *Electr. Eng. Diss.* **2008**, Paper 14.

29. Chaaban, M.A.; Alahmad, M.; Neal, J.; Shi, J.; Berryman, C.; Cho, Y.; Lau, S.; Li, H.; Schwer, A.; Shen, Z.; Stansbury, J.; Zhang, T. Adaptive photovoltaic system. In Proceedings of the IECON 2010—36th Annual Conference on IEEE Industrial Electronics Society, Glendale, AZ, USA, 7–10 November 2010; pp. 3192–3197.

30. Patnaik, B.; Sharma, P.; Trimurthulu, E.; Duttagupta, S.P.; Agarwal, V. Reconfiguration strategy for optimization of solar photovoltaic array under non-uniform illumination conditions. In Proceedings of the 2011 37th IEEE Photovoltaic Specialists Conference, Seattle, WA, USA, 19–24 June 2011; pp. 1859–1864.

31. Velasco-Quesada, G.; Guinjoan-Gispert, F.; Pique-Lopez, R.; Roman-Lumbreras, M.; Conesa-Roca, A. Electrical PV array reconfiguration strategy for energy extraction improvement in grid-connected PV systems. *IEEE Trans. Ind. Electron.* **2009**, *56*, 4319–4331.

32. Mohammadmehdi, S.; Mekhilef, S.; Rahmani, R.; Yusof, R.; Renani, E.T. Analytical modeling of partially shaded photovoltaic systems. *Energies* **2013**, *6*, 128–144.

33. Ciulla, G.; Brano, V.L.; Dio, V.D.; Cipriani, G. A comparison of different one-diode models for the representation of I–V characteristic of a PV cell. *Renew. Sustain. Energy Rev.* **2014**, *32*, 684–696.

34. Cipriani, G.; Dio, V.D.; Cascia, D.L.; Miceli, R.; Rizzo, R. A novel approach for parameters determination in four lumped PV parametric model with operative range evaluations. *Int. Rev. Electr. Eng.* **2013**, *8*, 1008–1017.

35. Jazayeri, M.; Uysal, S.; Jazayeri, K. A simple Matlab/Simulink simulation for PV Modules Based on One Diode Model. In Proceedings of the 2013 10th International Conference on High Capacity Optical Networks and Enabling Technologies, Magosa, Cyprus, 11–13 December 2013.

36. Celik, A.N.; Nasir, A. Modelling and experimental verification of the operating current of mono-crystalline photovoltaic modules using four-and five-parameter models. *Appl. Energy* **2007**, *84*, 1–15.

37. Skoplaki, E.; Palyvos, J. On the temperature dependence of photovoltaic module electrical performance: A review of efficiency/power correlations. *Sol. Energy* **2009**, *83*, 614–624.

38. De Soto, W.; Klein, S.A.; Beckman, W.A. Improvement and validation of a model for photovoltaic array performance. *Sol. Energy* **2006**, *80*, 78–88.

39. Armstrong, S.; Hurley, W.G. A thermal model for photovoltaic panels under varying atmospheric conditions. *Appl. Ther. Eng.* **2010**, *30*, 1488–1495.

40. Villalva, M.G.; Gazoli, J.R. Comprehensive approach to modeling and simulation of photovoltaic arrays. *IEEE Trans. Power Electron.* **2009**, *24*, 1198–1208.

41. Patel, H.; Agarwal, V. MATLAB-Based Modeling to Study the Effects of Partial Shading on PV Array Characteristics. *IEEE Trans. Energy Convers.* **2008**, *23*, 302–310.

42. David, L.; King, J.; Kratochvil, A.; Boyson, E. Measuring solar spectral and angle-of-incidence effects on photovoltaic modules and solar irradiance sensors. In Proceedings of the Conference Record of the Twenty-Sixth IEEE Photovoltaic Specialists Conference, Anaheim, CA, USA, 29 September–3 October 1997.

43. Moballegh, S.; Jiang, J. Partial shading modeling of photovoltaicsystem with experimentalvalidations. In Proceedings of the Power and Energy Society General Meeting, 2011 IEEE, San Diego, CA, USA, 24–29 July 2011.

44. Abete, A.; Barbisio, E.; Cane, P.; Demartini, P. Analysis of photovoltaicmodules with protectiondiodes in presence of mismatching. In Proceedings of the 1990 Conference Record of the Twenty First IEEE PhotovoltaicSpecialists Conference, Kissimmee, FL, USA, 21–25 May 1990.

45. Wang, Y.J.; Lin, S.S. Analysis of a partiallyshaded PV array considering different module connection schemes and effects of bypass diodes. In Proceedings of the 2011 International Conference and IEEE Utility Exhibitionon Power and Energy Systems: Issues & Prospects for Asia (ICUE), Pattaya, Thailand, 28–30 September 2011.

46. Shmilovitz, D.; Levron, Y. Distributed Maximum Power Point Tracking in Photovoltaic Systems—Emerging Architectures and Control Methods. *Automatika* **2012**, *53*, 142–155.